EAGE

PAS04

Low Frequency Passive Seismic Tomography using Valhall LoFS

A. Mordret* (Institut de Physique du Globe de Paris), N.M. Shapiro (Institut de Physique du Globe de Paris), S. Singh (Institut de Physique du Globe de Paris), P. Roux (LGIT, Grenoble) & O.I. Barkved (BP, Norway)

SUMMARY

We used 6 hours of vertical component continuous data recorded from more than 2400 receivers of the Valhall LoFS for passive seismic interferometry. The Correlation Functions contain symmetrical Scholte-waves in the 0.1-2 Hz frequency range and we showed by beamforming that the sources of these waves were homogeneously distributed around the array. We constructed group velocity dispersion curves of the extracted Scholte-waves and inverted them to produce a group velocity map of the Valhall field subsurface. We found that seismic velocities were higher in the center of the array than at its edge. It is in good agreement with geomechanical models based on the sea-floor subsidence due to the reservoir production.

Introduction

Several studies used the passive data from the Valhall LoFS ocean bottom network in order to apply passive seismic interferometry (Stewart, 2006; Artman, 2007; Dellinger, 2008; Dellinger and Yu, 2009). In this study, we assessed the spatial distribution of the seismic noise sources in different frequency bands; we showed, in agreement with Dellinger and Yu (2009), that the seismic noise was omnidirectional in the frequency range 0.1-2 Hz. We used this frequency band to retrieve the Scholte-wave part of the Green's function between Valhall sensors. Then, using this dataset, we were able to perform a Scholte-wave tomography of the Valhall area subsurface.

Data processing

We used 6 hours of continuous recording of the vertical component from more than 2500 4C geophones . The seismic noise pre-processing follows the procedure of Bensen (2007): a single-station processing (separation of the traces in 1-minute long segments, temporal normalisation and spectral whitening) followed by the correlation of each segment for all possible pairs of stations and the stack of all correlations with each pair of stations.

Figure 1A shows 300 Correlation Functions (CF) filtered between 0.1 and 2 Hz with inter-station distance ranging from 300 m to 2500 m. We clearly see a dispersive wave (Scholte-wave) with a moveout velocity at about 400 m/s. The stations used in figure 1A are all far away from the rig (a sub-array of 25 sensors about 4 km south-east from the rig used for the beamforming). However, when we computed CF from stations close to the rig (less than 2 km, figure1B) it appeared that there was no Scholte-wave synthesised during the correlation process in this frequency band. This may be due to the rig noise that overcomes the microseismic noise or to the gas cloud in the centre of the array that strongly attenuates seismic waves.

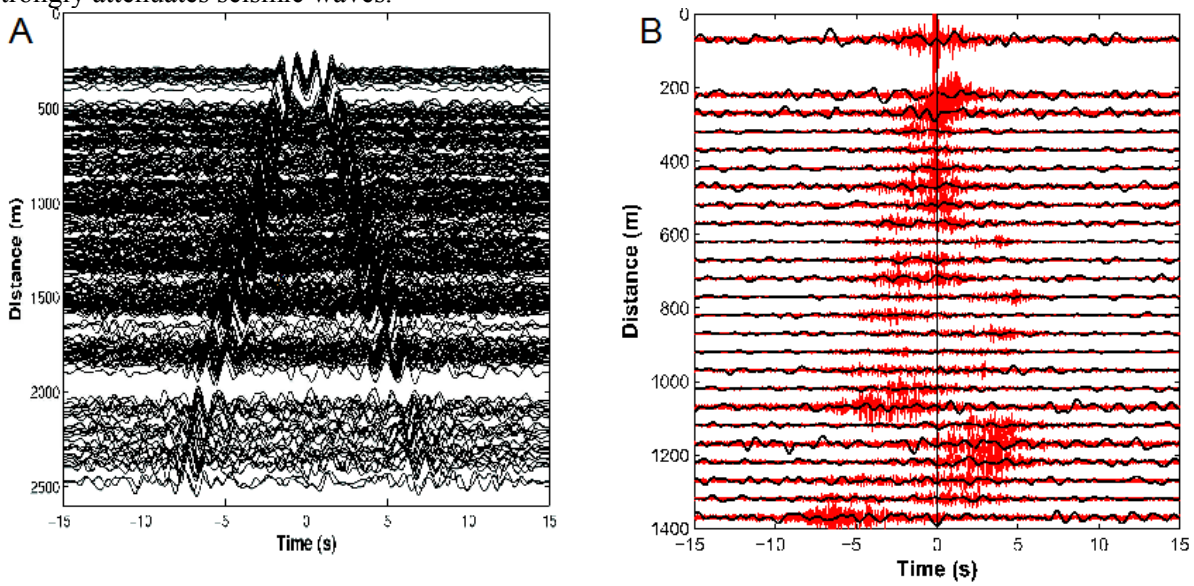

Figure 1 *A) 300 Correlation Functions filtered between 0.1 and 2 Hz sorted by increasing inter-station distance, 4 km from the rig in average. B) In red, non filtered CF close to the rig, in black, the same CF filtered between 0.1 and 2 Hz.*

Noise sources location

To assess the directivity of the waves that are reconstructed in the CF, we performed a beamforming analysis (e.g. Rost and Thomas, 2002) on the filtered CF of a 25-station sub-array with a distance of 4 km from the rig. This sub-array is made of three concentric circles with radii of 300 m, 600 m and 1200 m, centred on the station #1382, south-east of the rig, and the results of the beamforming are related to this position.

The results of the beamforming are shown on figure 2; they are represented in the slowness plan: each circle stands for the velocity specified nearby, the grey circle is for the velocity 1500 m/s, the acoustic wave-speed in water. The white plain and dotted-dashed lines show respectively the principal azimuth of the Valhall network and its perpendicular. The black straight line divide the space in 8 quadrants. We can see that in the 0.1-2 Hz range (figure 2A), the retrieved waves are omnidirectional (the orange circular shape) and arrive with a velocity close to 500 m/s whereas in the 20-40 Hz range (figure 2B), the waves arrive manly from the direction of the rig (from the North-East, the upper left corner of the figure) at 1500 m/s. Therefore, the waves extracted at 0.1-2 Hz which are dispersive waves (Dellinger and Yu, 2009) are more suitable to perform a surface-wave tomography. The linear patterns perpendicular to the main direction of the LoFS array are aliasing artifacts due to the uneven distribution of sensors.

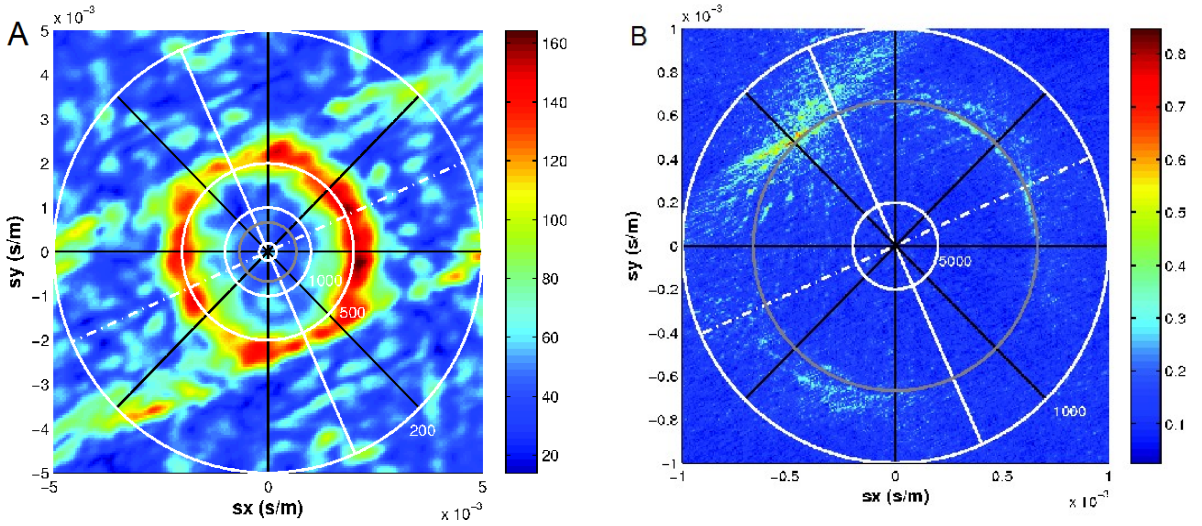

Figure 2 *A) Beamforming of the CF in the frequency range 0.1-2 Hz. B) Beamforming of the CF in the frequency range 20-40 Hz.*

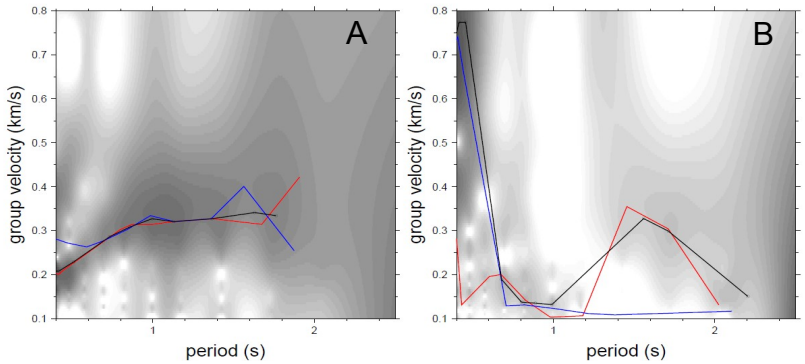

Figure 3 *A) Dispersion curves for a CF far away from the rig and kept for the tomography. B) Dispersion curves for a CF close to the rig and rejected for the tomography. The blue curves are the dispersion curves for the negative side of the CFs, the red ones are dispersion curves of the positive side of the CFs, the black ones are dispersion curves for the symmetric part of the CFs.*

Surface-wave tomography

We used more than 184 000 CF extracted from station pairs separated from 1 km to 1.5 km. We computed the dispersion measurements using a Frequency-Time Analysis (FTAN, Levshin et al. 1989) over the negative, positive and symmetric (the average between the negative and the positive lags) parts of the CF at 9 periods between 0.4 and 2 s when it was possible. Theoretically, the dispersion curves of both three parts of the CF should be identical, thus, we used the difference between the negative and positive measurements to estimate the errors on the group-velocity measurements. We kept only the most accurate dispersion curves, i.e. when the difference between the negative and positive dispersion curves were the smallest, that had had for consequence to remove most of dispersion curves made from stations closer than 2 km from the rig (figure 4A). The dispersion measurements of Scholte waves from 6 hours continuous data correlation were used to invert for group velocity maps on a 36 × 46 grid with 250 × 250 m cells size across the Valhall network using the surface-wave tomographic method of Barmin et al. (2001). Results at 0.8 s are shown on figure 4B.

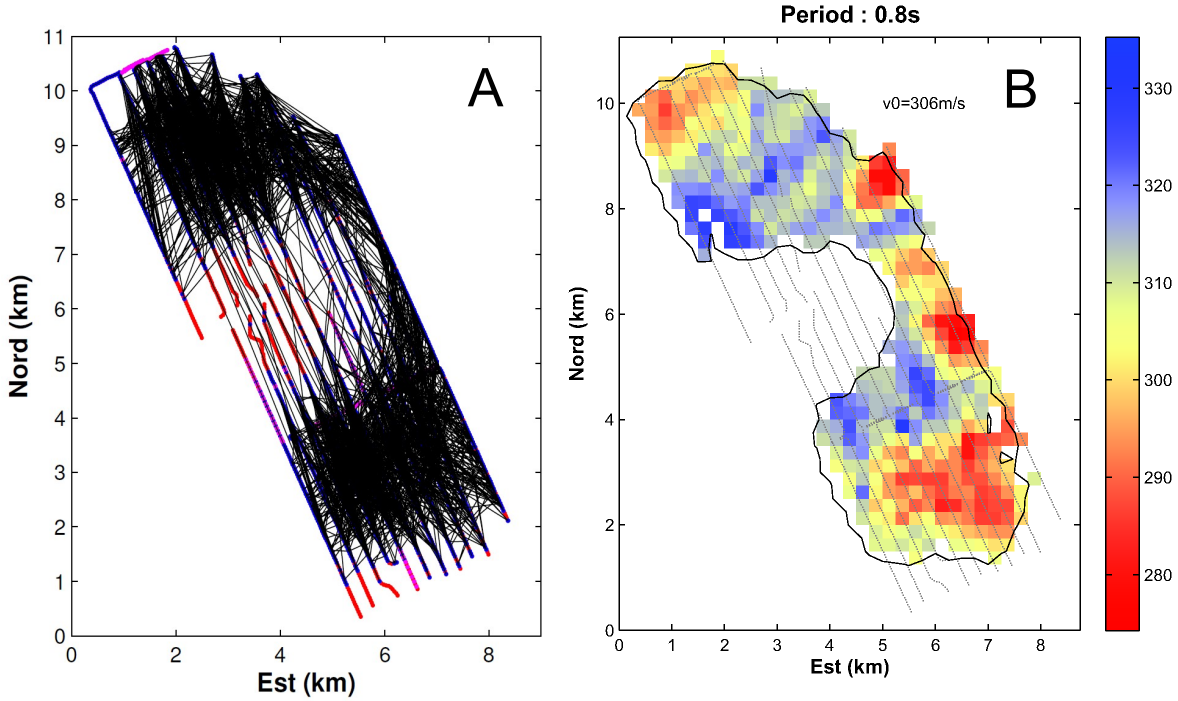

Figure 4 *A) Path coverage after removing the bad dispersion measurements at 0.8 s. Red points are stations polluted by the rig noise, magenta points non operational stations. B) Surface wave group velocity (m/s) tomography of the Valhall field subsurface at 0.8 s period.*

Discussion

Our results are best resolved at 0.8 and 1 s where data quality was best and where we could therefore keep the largest amount of data. Beside the lack of data near the rig, we observe a higher velocity in the centre of the field than at its periphery. This result is in very good agreement with Hatchell et al.'s (2009) results who showed Scholte wave velocity maps for different Valhall LoFS data vintages with the same pattern. Our results lead to the same interpretation. The reservoir compaction induced by the production creates a sea-floor subsidence. Geomechanical models (Hatchell et al., 2009) show that this subsidence creates horizontal strain that has a contractional component at the centre of the field whereas it turns to be extensional toward the edges of the field.

Thus, in areas where the sea-floor sediments are compressed the seismic velocity is high, whereas, where the sediments are stretched the velocity decreases. Landès et al. (2009), using passive seismic interferometry at higher frequency (between 3 and 12 Hz and between 24 and 29 Hz) found also a similar decreasing velocity trend moving away from the rig.

Conclusions

Using 6 hours of continuous records at Valhall LoFS nework, we performed a surface wave tomography based on seismic noise CF. We found higher velocities in the centre of the field where the strain due to production-induced subsidence is expected contractional and slower velocity on the edge of the field where strain is extensional.

These results are consistent with results obtain with more conventional studies using the active LoFS data vintage acquisition. However, this passive seismic technique allows such a study to be repeated much more often than the usual active ones and is virtually costless. These results can be useful to monitor reservoirs subsidence or better understand the strain and seismic velocity variations induced by reservoirs subsidence, they could help to construct more accurate geomechanical models or define precise S-wave statics. Moreover, we could imagine to make such analyses monthly or even weekly to better monitor the reservoir behaviour during production.

Acknowledgements

The authors wish to thank the Valhall partnership (BP Norge, Norske Shell, Total E&P Norge, and Amerada Hess Norge) for permission to publish this paper.

References

Artman, B., 2007. Passive Seismic Imaging, Ph.D. Thesis, Stanford Exploration Project report SEP-128, Stanford University, Stanford, California, USA.
Barmin, M., Ritzwoller, M., & Levshin, A., 2001. A fast and reliable method for surface wave tomography, Pure and Applied Geophysics, 158(8), 1351–1375.
Bensen, G., Ritzwoller, M., Barmin, M., Levshin, A., Lin, F., Moschetti, M., Shapiro, N., & Yang, Y., 2007. Processing seismic ambient noise data to obtain reliable broad-band surface wave dispersion measurements, Geophysical Journal International, 169(3), 1239–1260.
Dellinger, J., 2008. Low frequencies using conventional sensors: “sign-bit” recording revisited, 78th annual SEG meeting, Expanded Abstracts, 149–153, doi: 10.1190/1.3054777
Dellinger, J. and Yu, J., 2009. Low-frequency virtual point-source interferometry using conventional sensors, 71st EAGE Conference.
Hatchell, P.J., Wills, P.B. & Didraga, C., 2009. Production Induced Effects on Near-surface Wave Velocities at Valhall, 71st EAGE Conference, Paper T016.
Landès, M., Shapiro, N.M., Singh, S., & Johnston, R., 2009. Studying shallow seafloor structure based on correlations of continuous seismic records, 79th Annual SEG Meeting.
Levshin, A., Yanovskaya, T., Lander, A., Bukchin, B., Barmin, M., Ratnikova, L., & Its, E., 1989. Seismic surface waves in a laterally inhomogeneous Earth, Kluwer, Dordrecht.
Rost, S. & Thomas, C., 2002. Array seismology: methods and applications, Rev. Geophys, 40(3), 1008.
Stewart, P., 2006. Interferometric imaging of ocean bottom noise, 76th annual SEG meeting, Expanded Abstracts, 1555–1559, doi: 10.1190/1.2369817